# Dynamics in supercooled liquids and in the isotropic phase of liquid crystals: A comparison

Hu Cang, Jie Li, V. N. Novikov,[a] and M. D. Fayer
*Department of Chemistry, Stanford University, Stanford, California 94305*

(Received 14 January 2003; accepted 26 February 2003)

A comparison is made of the dynamics observed over wide ranges of time and temperature between five supercooled liquids and four isotropic phase liquid crystals that have been previously studied separately. Optical-heterodyne-detected optical Kerr effect (OHD–OKE) measurements were employed to obtain the orientational relaxation dynamics over time scales from sub-ps to tens of ns. For the supercooled liquids, the temperatures range from above the melting point down to $\sim T_c$, the mode coupling theory critical temperature. For the liquid crystals, the temperatures range from well above the isotropic-to-nematic phase transition temperature $T_{NI}$ down to $\sim T_{NI}$. For time scales longer than those dominated by intramolecular vibrational dynamics ($\gtrsim$1 ps), the fundamental details of the dynamics are identical. All nine liquids exhibit decays of the OHD–OKE signal that begin ($>$1 ps) with a temperature-independent power law $t^{-z}$, where $z$ is somewhat less than or equal to 1. The power law decay is followed in both the supercooled liquids and liquid crystals by a crossover region, modeled as a second power law. The longest time scale decay for all nine liquids is exponential. In supercooled liquids, the exponential decay is the $\alpha$ relaxation (complete structural relaxation). In liquid crystals, the exponential decay is the Landau–de Gennes decay (relaxation of pseudonematic domains). As $T_c$ (supercooled liquids) and $T_{NI}$ (liquid crystals) are approached from above, the time range over which the ''intermediate'' power law can be observed increases, until near $T_c$ and $T_{NI}$, the power law can be observed from $>$1 ps to many ns. The data for all nine liquids are described accurately by the same functional form and exhibit a scaling relation in common. The nature of the dynamics in the liquid crystals is understood in terms of pseudonematic domains that have a correlation length $\xi$, which increases as $T_{NI}$ is approached. It is conjectured that the similarities between the liquid crystal data and supercooled liquid data are produced by the same underlying physical features: that is, like liquid crystals, supercooled liquid dynamics is a result of structural domains even at relatively high temperature. © *2003 American Institute of Physics.* [DOI: 10.1063/1.1568338]

## I. INTRODUCTION

In spite of a vast number of experiments using a wide variety of techniques,[1–21] the microscopic dynamic nature of supercooled liquids is not understood on mesoscopic distance scales, that is, distances that are greater than a single molecule, but substantially less than a bulk sample. Very close to the glass transition temperature $T_g$, there have been a number of experiments that suggest supercooled liquids are structurally heterogeneous.[22,23] At higher temperatures, particularly above $T_c$, the mode-coupling theory (MCT) critical temperature ($\sim$20% above $T_g$), where even the slowest dynamics are relatively fast (on the order of 100 ns), there is little on which to base a picture of the structural characteristics that give rise to the complex dynamics observed in molecular supercooled liquids. Simulations on spheres[24,25] and somewhat more complex shapes[26–28] provide insights, but they cannot address whether the supercooled liquid inhomogeneity that is observed very close to $T_g$ persists at much higher temperatures and whether the inhomogeneity is important in determining dynamics well above $T_g$.

The dynamics of liquid crystals in their isotropic phase is also complex, occurring over a wide range of time scales.[29–34] However, unlike supercooled liquids, there is a well-defined mesoscopic-scale physical picture of nematogens in the isotropic phase,[31,32,35,36] and this physical picture informs the still-evolving theoretical description of liquid crystal dynamics.[32] Above but near the nematic–isotropic ($N$–$I$) phase transition temperature $T_{NI}$ ($T_{NI}<T<T_{NI}+\sim$50 K), orientational relaxation dynamics is strongly influenced by local structures (pseudonematic domains) that exist in the isotropic phase.[35,36] A great deal of experimental work has been done using both time and frequency domain methods to examine the relatively long-time-scale orientational relaxation that is dominated by the randomization of the pseudonematic domains.[29,31,37–43] Near the $N$–$I$ phase transition, the isotropic phase is nematically ordered on a distance scale defined by a correlation length $\xi$.[35,36] As the $N$–$I$ phase transition is approached from above, $\xi$ grows, becoming infinite in the nematic phase. On time scales of many nanoseconds to hundreds of nanoseconds, depending on the temperature, the local order randomizes, giving rise to exponential decays in time domain optical Kerr effect experiments.[31,33,37]

[a]On leave from the Institute of Automation and Electrometry of the Russian Academy of Science, Novosibirsk, 630090, Russia.

 

The long-time-scale relaxation of the local structures is described by Landau–de Gennes (LdG) theory, which was formulated a number of years ago to account for affects on dynamics as the $N-I$ phase transition is approached from above and to describe nematiclike order above the phase transition.[35] The $N-I$ phase transition is weakly first order, and it has a noticeable influence on properties of the liquid near $T_{NI}$. LdG theory predicts the temperature dependence of long-time exponential decay in the isotropic phase, which has a sharply increasing decay time as the transition temperature is approached. LdG theory has been confirmed many times experimentally using techniques such as the optical Kerr effect,[29,31,37] depolarized light scattering,[38] dynamic light scattering,[39] magnetic[40] and electric[41] birefringence, and dielectric relaxation.[42,43] The influence of the pseudonematic domains on the long-time-scale dynamics continues to $>50$ K above the $N-I$ phase transition temperature.[31] LdG theory gives the correlation length as

$$\xi(T)=\xi_0[T^*/(T-T^*)]^{1/2}, \tag{1}$$

where $\xi_0$ is a molecular length scale (typically 7–8 Å) and $T^*$ is a temperature 0.5–1.0 K lower than $T_{NI}$.[36] (Properties scale as $T^*$ is approached rather than $T_{NI}$ because the phase transition has both first- and second-order character.) At sufficiently high temperature, the size of the domains becomes similar to the molecular volume, and LdG theory ceases to apply.

On time scales short compared to the time for pseudonematic domain randomization and on distance scales short compared to $\xi$, nematogens exist in an environment with nematiclike order. Dynamics on short time scales (less than a few ns) are not described by the LdG theory. The dynamics is strongly influenced by the local order. A number of studies in the past decade have investigated orientational relaxation dynamics in the short-time regime.[30,31,44–47] Recently, improvements in experimental technique have made it possible to examine the full time dependence as a function of temperature.[32–34] The experiments use the optical-heterodyne-detected optical Kerr effect (OHD–OKE) to study the dynamics from $<1$ ps to hundreds of ns with excellent data over the full time range. The experiments were conducted from well above $T_{NI}$ down to $\sim T_{NI}$. The OHD–OKE experiment measures the time derivative of the polarizability–polarizability correlation function[48–51] (equivalent to the time derivative of the orientational correlation function, except on $<1$ ps time scales).

The experiments reported previously on four liquid crystals observe temperature-independent power law decays at short times and the LdG exponential decay at long times.[32–34] A preliminary theoretical analysis that calculates the orientational correlation function on fast time scales, based on a description of the collective orientational relaxation, has been presented.[32] The theoretical correlation function is not a power law, but its derivative displays a power-law-like decay at short time.[32]

Between the short-time-scale power law and the long-time-scale LdG exponential decay, there is a crossover region. This region has been modeled as another exponential decay.[32–34] However, because of its low amplitude and short time span, the crossover region can be equally well modeled as a second power law (see below). This crossover power law is akin to the MCT von Schweidler power law.

Mode coupling theory provides a reference frame for the discussion of the dynamics of supercooled liquids and comparison with liquid crystals. Some of the basic features of the experimental observations are reasonably well described by the two-step case of MCT at temperatures well above $T_g$.[52,53] In the MCT description, the time dependence of the density–density correlation function (and the orientational correlation function[26–28]) consists of a fast temperature-independent decay (the critical decay or fast $\beta$ process) followed by a curve with complex shape that obeys a temperature-dependent time scaling relation. This curve eventually decays to zero through complete structural relaxation. The earliest component of the complete structural relaxation decays as a power law, the von Schweidler power law, followed by an exponential or approximately exponential decay, the slow $\alpha$ process. As the temperature is lowered from high temperature, the relaxation time of the $\alpha$ process lengthens dramatically, and according to ideal MCT, it diverges at $T_c$, at which all fluctuations are frozen.[52,53]

However, recent detailed experimental studies of five supercooled liquids[19] demonstrate that the short-time-scale dynamics ($\sim$1 ps to 1–10 ns, depending on the temperature) does not correspond to the dynamics predicted by the MCT standard model. Rather than the functional form of the decay predicted by MCT, a power law $t^{-z}$, with temperature-independent exponent $z$, is observed.[19] The values of $z$ are equal to or somewhat less than 1. This power law has been called the intermediate power law because, in the language of MCT, it falls between the critical decay (fast $\beta$ process) and the von Schweidler power law. The temperature-independent power law is followed by the von Schweidler power law and then the exponential $\alpha$ relaxation. Certain scaling relations predicted by MCT are obeyed.[19]

The fundamental point of this paper is that the nature of the dynamics observed in the isotropic phase of liquid crystals and in supercooled liquids is essentially identical. On time scales sufficiently long such that the observations are not dominated by intramolecular vibrational degrees of freedom ($\gtrsim$1 ps), both types of liquids decay with a temperature-independent power law, followed by a crossover region, which can be described as a second power law. The final, complete structural relaxation is a highly temperature-dependent exponential decay. The data for all nine liquids that were previously studied separately, five supercooled liquids[16–19] and four liquid crystals,[32–34] are fit here with the identical fitting function. While the parameters that describe the various liquids differ, they differ among the liquids of a single type as well as between supercooled liquids and liquid crystals. The main difference in the parameters is that the liquid crystals have a power law exponent $z$, which is dependent on the aspect ratio of the nematogen. When $z$ for the liquid crystals is extrapolated to an aspect ratio of 2.5, the ratio below which liquids no longer behave as liquid crystals, the value is in the range of $z$'s found for the supercooled liquids.

The similarities in the dynamical behavior of the supercooled liquids and the liquid crystals suggest that a similar underlying molecular nature of the liquids gives rise to the dynamics. The dynamics in liquid crystals in the isotropic phase is determined by the pseudonematic domain structure of the liquid. The correlation length of the domains increases as $T_{NI}$ is approached from above. The results bring out the possibility that supercooled liquids could behave as they do because they also have a type of domain structure, even at relatively high temperatures, that grows as the temperature is lowered. However, unlike liquid crystals, supercooled liquids do not go through a structural phase transition.

## II. EXPERIMENTAL PROCEDURES

The results that will be discussed below have been presented previously.[16–19,34] However, because the essential point here is to compare the results of experiments on two types of liquids, it is important to describe the nature of the experimental procedures, if only briefly.

The five supercooled liquids studied are benzophenone (BZP),[19] and 2-biphenylmethanol (BPM),[19] ortho-terphenyl (OTP),[17] salol,[16] and dibutylphthalate (DBP).[18] The four liquid crystals studied are 4′-(phentyloxy)-4-biphenylcarbonitrile (5-OCB), 4′-phentyl-4-biphenylcarbonitrile (5-CB) and 1-isothiocyabato-(4-propylcyclohexyl)benzene (3-CHBT),[32,33] and 4′-Octyl-4-biphenylcarbonitrile (8-CB).[34]

The supercooled liquid samples were prepared as follows: Sample cuvettes (1 cm optical length) were cleaned on a distillation apparatus to remove dust and other contaminates. The materials were purchased from Aldrich and were purified by fractional vacuum distillation and sealed in the optical cuvettes while still attached to distillation apparatus. This procedure removed dust that could act as nucleation sites for crystallization. The liquid crystal materials were also purchased from Aldrich and used without further purification except for filtration through a 0.2-$\mu$m disk filter to reduce scattered light. The samples were sealed under vacuum in 1-cm glass cuvettes. Temperature control was obtained using a constant-flow cryostat, with temperature stability of $\pm 0.1$ K.

The optical heterodyne detected optical Kerr effect experiment, a nonresonant pump–probe technique,[54,55] measures the time derivative of the polarizability–polarizability correlation function (orientational correlation function).[56,57] The pump pulse induces an optical anisotropy. The induced optical anisotropy decays because of orientational relaxation. The decay is measured with a time-delayed probe pulse. The Fourier transform of the OHD–OKE signal is directly related to data obtained from depolarized light scattering,[58,59] but the time domain OHD–OKE experiment can provide better signal-to-noise ratios over a broader range of times for experiments conducted on very fast to moderate time scales.

When sufficiently short excitation pulses are used ($\leqslant$70 fs), the correspondingly large bandwidth excites an orientationally anisotropic distribution of librations via stimulated Raman scattering. The damping of the optically excited librations leaves behind a residual molecular orientational alignment. When the excitation pulses are longer, the corresponding bandwidth is insufficiently broad to drive librational motions by stimulated Raman scattering. Rather, the **E** field associated with longer pulses exerts a torque on anisotropic polarizable molecules, which results in a molecular orientational anisotropy along the direction of the applied **E** field. In either case, the resulting orientational anisotropy gives rise to an optical birefringence in the sample, which is monitored by the probe pulse. A pulsed probe beam, in conjunction with two delay lines (0–600 ps and 0–30 ns), was used for monitoring decays up to 30 ns. For longer decay times, following pulsed excitation, a cw probe beam and a fast digitizer were employed to measure the decay.

A Ti:sapphire oscillator and 5-kHz regenerative amplifier provided the pulses. An adjustable grating compressor permitted pulse durations of from $<$70 fs to 2 ps [full width at half maximum (FWHM)] to be obtained. The longer pulses are achieved by incomplete compression. In addition, bypassing the grating compressor entirely yields pulses of $\sim$100 ps FWHM. The partially compressed and uncompressed pulses are chirped. The use of chirped pulses does not interfere with the production or detection of the optical Kerr effect because it is a nonresonant experiment. The shortest pulses were used to resolve the fastest-time-scale data. Better signal-to-noise ratios were obtained at long times by using longer pulses with greater average power. The cw probe was obtained from a commercial diode laser, centered at 635 nm, with an output power of 15 mW.

Data were collected over four distinct time ranges: 0–20 ps using 70-fs pulses and a 0.1-$\mu$m stepper motor delay line; 3–600 ps using 1-ps pulses and a 0.1-$\mu$m stepper motor delay line; 0.1–30 ns using 100-ps pulses and a 30-ns delay line; and 2 to several hundred ns using 100-ps pump pulses, a cw probe, and a fast digitizer. The significant overlap of each time range with the next longer range permitted the data sets to be merged by multiplication of the data amplitude until decays were coincident in the overlap region. Care was taken to ensure data overlap between differing time scales was excellent.

## III. COMPARISON OF SUPERCOOLED LIQUID AND LIQUID CRYSTAL RESULTS

Figure 1 displays data on logarithmic plots for one of the supercooled liquids, BZP, and one of the liquid crystals, 5-OCB. The plots begin at 1 ps. At shorter times, the data are strongly influenced by the excitation of intramolecular vibrational modes that give rise to oscillatory signals.[16] Some of the oscillatory character is still visible in the BZP data between 1 and 2 ps. All of the data for the five supercooled liquids and the four liquid crystals have the same general appearance that is displayed in Fig. 1. As will be shown below, all of the data sets for $t \gtrsim 1$ ps can be decomposed into three parts. The shortest time portion is a power law, the ''intermediate'' power law. It is called intermediate because it follows the ultrafast dynamics and precedes the longer-time-scale full structural relaxation. The ultrafast dynamics have the intramolecular vibrational oscillations superimposed on a decay that is referred to in MCT as the critical decay or fast $\beta$ process.[52,53,60,61] The ultrafast portions of the

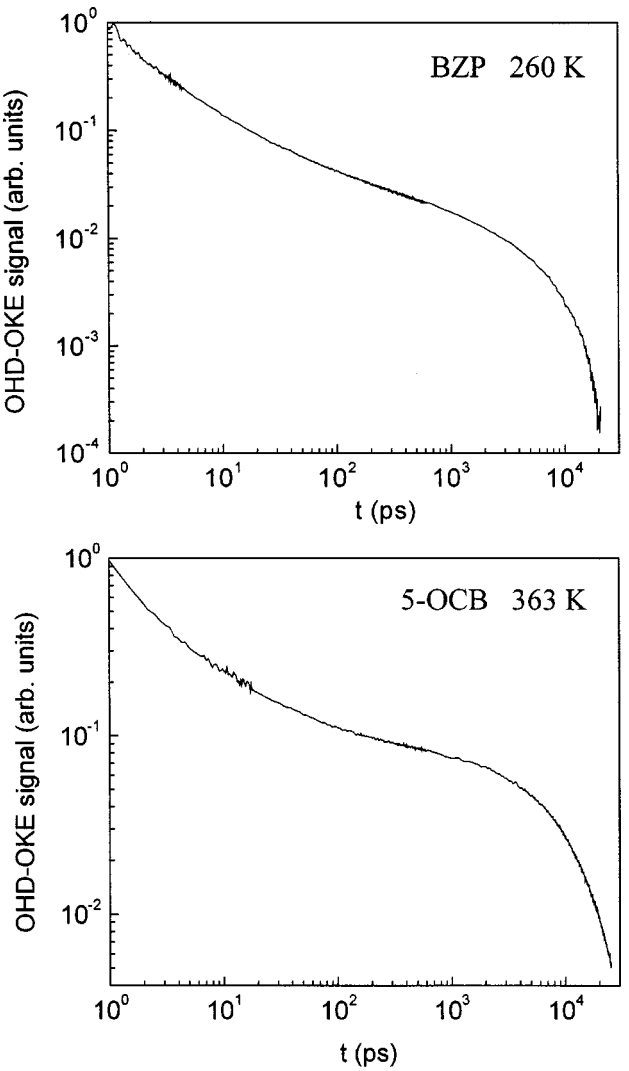


FIG. 1. Typical data on logarithmic plots for one of the supercooled liquids, benzophenone (BZP), and one of the liquid crystals, 4′-(phentyloxy)-4-biphenylcarbonitrile (5-OCB) from 1 ps to >20 ns. In each plot, the short-time portions are power laws. The long-time portions are exponential decays. In between, there is a crossover region.

data are not considered hear because they span a very short observable time range and the data are substantially obscured by the intramolecular vibrations.[16]

On the longest time scale, the data are single exponential decays. These are the portions of the data in Fig. 1 that appear as a steep drop after a few ns. Between the intermediate power law and the final exponential decay there is a crossover region with different functional form. In supercooled liquids, this region is generally described as a power law, the von Schweidler power law. In the experiments on liquid crystals, the crossover region was modeled as another exponential.[32–34] However, in supercooled liquids the crossover region spans only a short time and is of low amplitude. In the liquid crystals, the crossover region spans a longer time. In both types of liquids, the exact functional form of the crossover region is difficult to determine. The form used to fit the liquid crystal data[32–34] has an additional adjustable parameter and gives a slightly better fit. For consistency with the literature on supercooled liquids and the previous OHD–OKE experiments on supercooled liquids discussed here,[16–19] the crossover region in the liquid crystals is modeled as a power law. As discussed below, all of the liquid crystal data were refit with the same function used to describe the supercooled liquids.

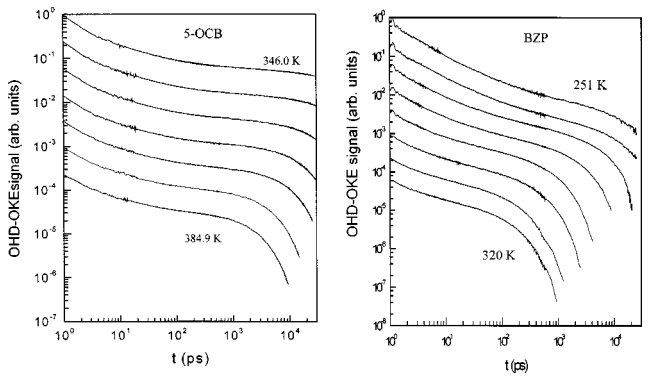


FIG. 2. Temperature-dependent data for one of the liquid crystals, 5-OCB, and one of the supercooled liquids, BZP. The supercooled liquid data cover a temperature range from well above $T_c$ to $\sim T_c$. The liquid crystal data cover a temperature range from well above $T_{NI}$ to $\sim T_{NI}$. The curves have been offset for clarity of presentation. Starting with the topmost curve, the temperatures for the 5-OCB data sets are 346.0, 348.0, 352.1, 357.0, 363.0, 374.9, and 384.9 K. Starting with the topmost curve, the temperatures for the BZP data sets are 251, 254, 260, 269, 281, 290, 302, 311, and 320 K. The temperature-dependent data sets for all nine liquids have similar appearances. The major temperature dependence is the slowing of the long-time-scale exponential relaxation as $T$ is decreased.

Figure 2 displays temperature-dependent data for one of the supercooled liquids, BZP, and one of the liquid crystals, 5-OCB. The supercooled liquid data cover a temperature range from well above $T_c$ to $\sim T_c$. The liquid crystal data cover a temperature range from well above $T_{NI}$ to $\sim T_{NI}$. The curves have been offset for clarity of presentation. The temperatures are given in the figure caption. Qualitatively, the data have the same type of temperature dependences, which will be shown to be true quantitatively below. The major changes with temperature are the long-time-scale exponential relaxations. As the temperature is increased, the exponential decays become faster (decay constants $\tau_\alpha$ for the supercooled liquid $\alpha$ relaxation and $\tau_{\mathrm{LdG}}$ for the Landau–de Gennes relaxation of the pseudonematic domain). The increased rates of the exponential decays reduce the time range over which the shorter-time-scale portions of the data can be observed. The short-time portions of the data do not change with temperature except in their amplitudes.

Over the wide ranges of temperatures investigated, the data for each of the five supercooled liquids and the four liquid crystals were fit for $t \gtrsim 2$ ps using the fitting function[19]

$$F(t) = [pt^{-z} + dt^{b-1}]\exp(-t/\tau). \tag{2}$$

The first term with $z \leqslant 1$ corresponds to the intermediate power law; the second term is the crossover power law (von Schweidler power law) with values of $b$ varying between 0.73 and 0.97; the exponential function describes the final $\alpha$-relaxation decay (supercooled liquids, $\tau_\alpha$) or the LdG decay (liquid crystals, $\tau_{\mathrm{LdG}}$). The product of the von Schweidler power law and the exponential has been previously shown to describe the longer-time portion of the

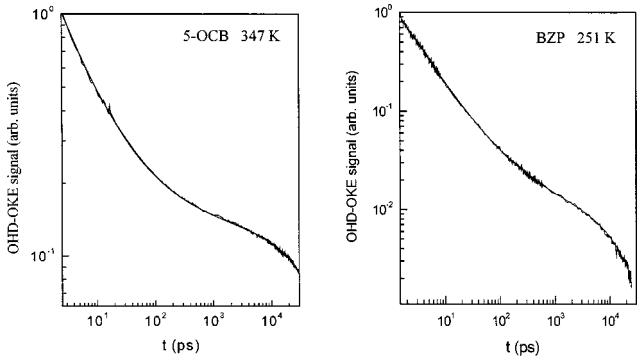


FIG. 3. Data and fits to Eq. (2) for one liquid crystal data set (5-OCB) and one supercooled liquid data set (BZP). The calculated curves fit both data sets very well. This is true for all nine liquids at all temperatures. Only the beginnings of the long-time portions of the data are shown so that the shorter-time data can be seen more clearly.

OHD–OKE data for the supercooled liquids extremely well.[16–19] Frequently, the longest-time portion of the correlation function, following the von Schweidler power law, is described as a stretched exponential. The optical OKE experiments measure the time derivative of the correlation function. The time derivative of a stretched exponential yields a product of a power law times a stretched exponential. Using a stretched exponential adds another power law and more parameters to the fit. We found that employing the time derivative of a stretched exponential did not improve the fits. For the liquid crystals, the LdG theory[36] and experiments[29,31,37] show the long-time decay is exponential. Therefore, we use an exponential decay for the longest-time portion of the data. Furthermore, the form used to fit the longest-time-scale relaxation, provided a good fit is obtained, does not influence the fit of the intermediate power law at much shorter times.

Figure 3 displays data and fits to Eq. (2) for one supercooled liquid data set (BZP) and one liquid crystal data set (5-OCB). The calculated curves describe both types of data very well. This is true for all nine liquids at all temperatures. In Fig. 3, only the beginnings of the long-time portions of the data are shown so that the shorter-time data can be seen more clearly. Figure 4 shows examples of the long-time exponential decays for one supercooled liquid (OTP) and one liquid crystal (3-CHBT) on semilogarithmic plots. The plots also have lines through the data. As can be seen for these two examples and is true of all of the liquids at all temperatures, the long-time portions of the decays are single exponentials.

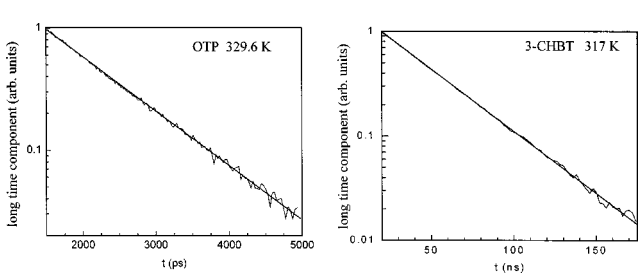


FIG. 4. Examples of the long-time exponential decays for one supercooled liquid, ortho-terphenyl (OTP), and one liquid crystal, 1-isothiocyabato-(4-propylcyclohexyl)benzene (3-CHBT), on semilogarithmic plots. The lines through the data sets show that the long-time portions of the decays are single exponentials. This is true of all of the liquids at all temperatures.

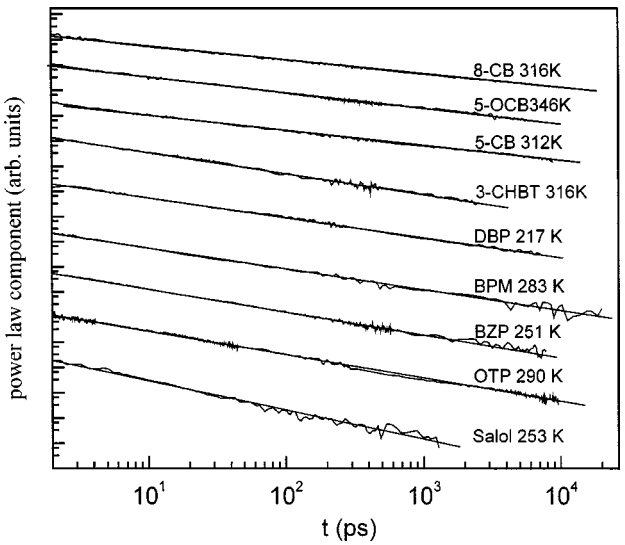


FIG. 5. Logarithmic plots of the power law portions of the data for the all nine liquids with the contributions from the long-time-scale exponential relaxation and the crossover region removed. The top four lines are the liquid crystals. The bottom five lines are the supercooled liquids. The data are straight lines (power laws) over three to four decades of time.

Figure 5 displays logarithmic plots of the intermediate power law portions of the data for all nine liquids with the contributions from the crossover term and the long-time-scale exponential relaxation removed. The top four lines are the liquid crystals. The bottom five lines are the supercooled liquids. The data are straight lines (power laws) over three to four decades of time. For each liquid at all temperatures, temperature-independent intermediate-time-scale power law decays are seen. Figure 5 clearly displays the nature of the intermediate power law portion of the decays. The intermediate power law exponent in the OHD–OKE experiment is $z$ [see Eq. (2)]. The value of $z$ for each liquid is given in Table I. The power laws only differ in their exponents. The figure is arranged with the largest exponent $z$ on the bottom and the smallest exponent on the top. The values of the exponents are discussed further below.

One of the key features of the data for all nine liquids is that the intermediate power laws have power law exponents that are temperature independent. Figure 6 displays the intermediate power law portion of the data on logarithmic plots at several temperatures for one supercooled liquid (BPM) and

TABLE I. Power law exponent ($z$), aspect ratio, and transition temperatures.

| | $z$ | Aspect ratio | $T_C$ (K) | $T_{NI}$ (K) |
|---|---|---|---|---|
| BZP | 0.87±0.03 | 1.81 | 250±4 | |
| BPM | 0.9±0.03 | 1.407 | 290±4 | |
| Salol | 1±0.03 | 2.11 | 260±4 | |
| OTP | 0.85±0.03 | 1.05 | 290±4 | |
| DBP | 0.79±0.03 | 1, 2* | 234±4 | |
| 8-CB | 0.54±0.02 | 4.56 | | 313±2 |
| 5-CB | 0.66±0.02 | 3.71 | | 308±2 |
| 5-OCB | 0.63±0.02 | 3.98 | | 344±2 |
| 3-CHBT | 0.78±0.02 | 3.26 | | 311.5±2 |

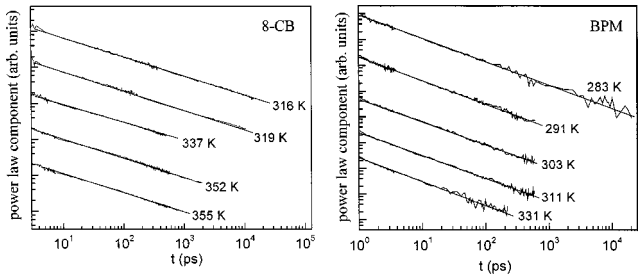


FIG. 6. Power law portion of the data at several temperatures for one liquid crystal, 8-CB, and one supercooled liquid, BPM, on logarithmic plots. Within experimental error, the lines in each plot have the same slopes. While the power law exponents vary from molecule to molecule (see Table I), in all cases for a given molecule the exponent is temperature independent.

one liquid crystal (8-CB). Within experimental error, for a given molecule, the lines in each plot have the same slopes. While the power law exponents vary from molecule to molecule (see Table I), in all cases the exponents are temperature independent. Although the power law exponents are not temperature dependent, the amplitudes of the intermediate power law portions of the decays are temperature dependent. Figure 7 displays the temperature dependence of the amplitude $p$ of the intermediate power law term [Eq. (2)] for four of the supercooled liquids and one of the liquid crystals. The temperature dependences for the supercooled liquids are shown in terms of the reduced temperature $(T-T_c)/T_c$ so that all of the data can be displayed on a single graph. For the liquid crystal, the plot is in terms of the regular temperature, which does not influence the comparison between the two types of liquids. To obtain $p$ at each temperature, the data sets were normalized to the peak of the electronic polarization contribution to the signal, which is temperature independent and only occurs at $t \cong 0$.[16] The normalization corrects for changes

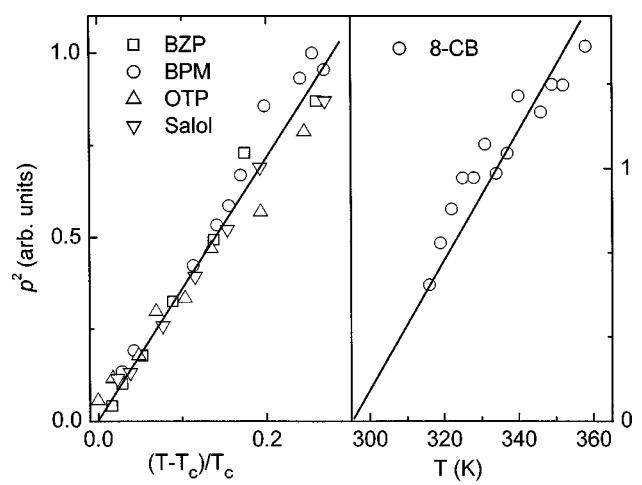


FIG. 7. Temperature dependence of the amplitude $p$ (plotted as $p^2$) of the intermediate power law term [Eq. (2)] for four of the supercooled liquids (BZP, BPM, OTP, salol) and one of the liquid crystals (8-CB). The temperature dependences for the supercooled liquids are shown in terms of the reduced temperature $(T-T_c)/T_c$ so that all of the data could be displayed on a single graph. For the liquid crystal, the plot is in terms of the regular temperature, which does not influence the comparison between the two types of liquids. Within experimental error, both the supercooled liquids and the liquid crystal have the same $\sqrt{T}$ temperature-dependent amplitude of the power laws.

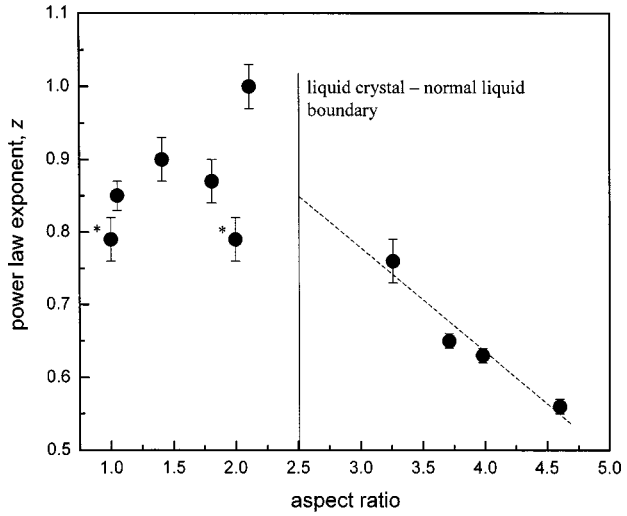


FIG. 8. Plots the power law exponents $z$ [see Eq. (2)] vs the molecular aspect ratio. The values are given in Table I. DBP is plotted twice (points indicated with $*$) because the aspect ratio is uncertain. The vertical line at 2.5 indicates the boundary between normal liquids ($<2.5$) and liquid crystals ($>2.5$). The liquid crystals display a clear dependence of the power law exponent on the aspect ratio. The supercooled liquids do not show a well-defined trend with aspect ratio.

in laser intensity and other parameters that influence the absolute size of the signal over the several days or weeks during which the data were collected. The necessary electronic polarization data were not available for one of the supercooled liquids, DBP, and for three of the liquid crystals. The liquid crystal data covers a limited range of temperatures because of the isotropic to nematic phase transition temperature. The higher-temperature data for both types of liquids have more scatter because the power law component becomes increasingly more difficult to separate from the slower portions of the data as the temperature is increased and the exponential decay becomes fast. The data are plotted as $p^2$, and the points fall on straight lines. Therefore, within experimental error, the supercooled liquids and the liquid crystal display the same $\sqrt{T}$ temperature dependence for the amplitude of the intermediate power law.

Figure 8 plots the intermediate power law exponents ($z$) versus the molecular aspect ratio. DBP is plotted twice because the aspect ratio is uncertain. Molecular modeling produced two reasonable structures. The two possible DBP data points are indicated with asterisks. Theoretical calculations demonstrate that molecules with aspect ratios $\lesssim 2.5$ will not behave as liquid crystals.[62] This boundary is indicated by the vertical line on the graph. The liquid crystals display a clear dependence of the intermediate power law exponent on the aspect ratio. As the aspect ratio becomes smaller, the value of the exponent becomes larger. The supercooled liquids do not show a well-defined trend with aspect ratio. For the supercooled liquids, the power law exponents vary from $\sim 1$ to $\sim 0.8$. A line is drawn through the liquid crystal points in Fig. 8 to indicate the value the power law exponent would take on at the boundary value of the aspect ratio. There is no theoretical basis for a linear extrapolation; it is only meant here to give an idea of what the power law exponent would be once the molecules can no longer form a liquid crystal phase.

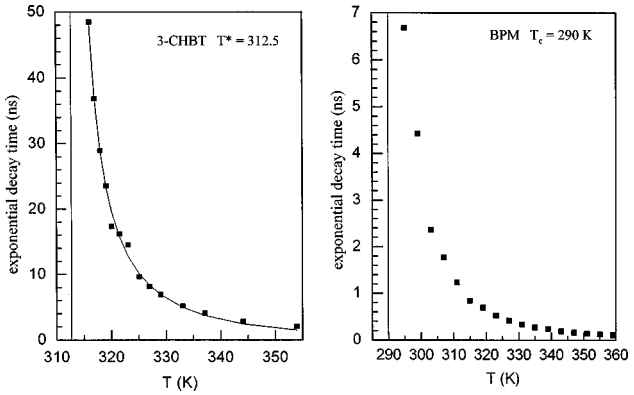


FIG. 9. Temperature dependence of the long-time-scale exponential relaxation decay time constants for one of the liquid crystals, 3-CHBT, and one of the supercooled liquids, BPM. The vertical lines indicate $T^*$ (liquid crystal) and $T_c$ (supercooled liquid). The analogous data for the other samples behave in the same manner. The line through the liquid crystal data is the LdG theoretical curve [Eq. (3)].

The line extrapolates to a value of 0.85, which falls in the middle of the observed range of values for the supercooled liquids.

Figure 9 displays temperature dependence of the long-time-scale exponential relaxation decay time constants for one of the liquid crystals, 3-CHBT, and one of the supercooled liquids, BPM. The analogous data for the other samples behave in the same manner. The line through the liquid crystal data is the LdG theoretical curve. LdG theory predicts that the domain randomization in the isotropic phase is described by an exponential decay function with the relaxation time $\tau_{\mathrm{LdG}}$, which diverges at the transition temperature $T^*$ as[36]

$$\tau_{\mathrm{LdG}} \propto \frac{V_{\mathrm{eff}}^* \eta(T)}{T - T^*}, \tag{3}$$

where $\eta(T)$ is the viscosity, $T$ is the temperature, and $V_{\mathrm{eff}}^*$ is the nematogens effective volume. The vertical line on the 3-CHBT panel marks the value of $T^*$. In all of the liquid crystals, $\tau_{\mathrm{LdG}}$ displays the same temperature-dependent behavior.

The BPM supercooled liquid data in Fig. 9 have much the same appearance as the liquid crystal data. The vertical line marks the value of the MCT critical temperature $T_c$, which was obtained using ''rectification diagrams'' that are based on MCT scaling relationships.[19] In ideal MCT, $T_c$ was thought to represent the glass transition. The structural relaxation ($\alpha$ relaxation) that gives rise to the long-time-scale exponential decay is arrested at $T_c$ according to MCT. Therefore, $\tau_\alpha$ should diverge at $T_c$. However, experiments demonstrate that $T_c$ is typically 20% higher in temperature than the glass transition temperature $T_g$. While $\tau_\alpha$ increases very rapidly as $T_c$ is approached, experiments show that it continues to increase as the temperature passes through $T_c$ from above.[16]

## IV. DISCUSSION

The liquid crystal samples are in their isotropic phase. Therefore, prior to the application of the excitation pulse's electric field, a sample is macroscopically isotropic. However, the LdG theory describes the system in terms of pseudonematic domains that have local nematic order over a correlation length $\xi$ [see Eq. (1)]. The long-time-scale exponential relaxation is the decay of the local nematic order. The short-time-scale power law decay and the crossover region occur on times fast compared to the loss of local nematic order. The short-time-scale dynamics reflects structural fluctuations on a time scale short compared to $\tau_{\mathrm{LdG}}$ and a distance scale short compared to $\xi$.

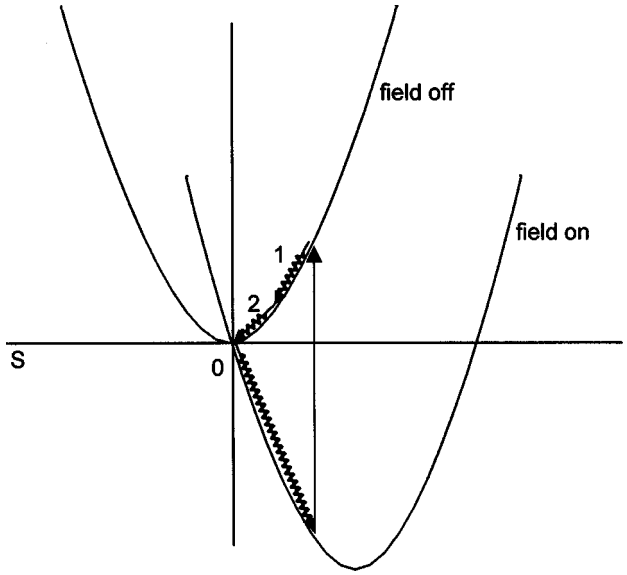


FIG. 10. Schematic illustration of the OHD–OKE experiment for a macroscopic liquid crystal sample. Initially, the order parameter $S=0$, the minimum of the free energy surface (field off). When the field is applied, the potential surface shifts (field on); the system is driven to align under the influence of the field. During the pulse, the system evolves along the new surface. When the field is removed, the potential returns to the field off surface. This leaves the system with $S\neq 0$, not at the bottom of the well. Application of the **E** field induces an anisotropy. Evolution will now occur on the surface to re-establish $S=0$. Relaxation of the induced anisotropy has two components: (1) intradomain relaxation giving rise to the fast power law decay and (2) pseudonematic domain randomization giving rise to the slow exponential decay described by Landau–de Gennes theory.

Figure 10 illustrates schematically the manner in which the field induces an anisotropy and why the two distinct relaxation processes can be observed. Initially, the macroscopic order parameter $S$ is zero. Application of the **E** field induces an anisotropy. The system begins at $S=0$, the minimum of the free energy surface. When the field is applied, the potential surface shifts; the system is induced to align under the influence of the field. During the pulse, the system evolves along the new surface (downward squiggly arrow). When the field is removed, the potential returns to the field-free surface. This leaves the system with $S\neq 0$, not at the bottom of the well (vertical arrow). Evolution will now occur on the field free surface to re-establish $S=0$.

To gain further insight, it is necessary to consider the problem microscopically.[44] There are two contributions to the relaxation illustrated in Fig. 10: intradomain relaxation (1) and domain randomization (2). The **E** field induces a small net alignment of the nematogens along the **E**-field direction. On a short distance scale ($<\xi$) the pseudonematic

order can be characterized by a local order parameter $S_\ell$. The **E**-field-induced molecular alignments change the local order parameter. Unlike $S$, which is a macroscopic parameter, $S_\ell$ is nonzero prior to the application of the optical field. $S_\ell$ defines the local nematic structure relative to the local director associated with a given pseudonematic domain. Initially, $S_\ell = S_\ell^0$. Immediately following the application of the field, $S_\ell \neq S_\ell^0$. The alignment of the molecules with the field not only changes $S_\ell$, but also results in the rotation of the local director toward the field. Fast intradomain relaxation occurs (power law signal decay), restoring the local order parameter to $S_\ell^0$. The restoration of $S_\ell^0$ does not return the nematogens to their initial spatial configurations. Rather, it returns the system to a local minimum of the potential surface. Because the nematogens were pulled toward the **E**-field direction, restoration of $S_\ell^0$ produces a local director that is somewhat aligned with the field direction. Because the local directors are to some extent aligned with the field, the macroscopic system still has an orientational anisotropy in spite of the fact that the intradomain fast relaxation has occurred. This long-lived anisotropy decays by randomization of the domains and is responsible for the multi-ns decay described by the LdG theory. Following the final LdG decay, the liquid still has pseudonematic order on a distance scale small compared to $\xi$ because of the nature of the intermolecular potential; however, the directions of the local directors have randomized. Returning to Fig. 10, the first part of the relaxation (labeled 1) is intradomain dynamics reestablishing the local order parameters to $S_\ell^0$. The final part of the macroscopic relaxation (labeled 2) is domain randomization that returns the macroscopic order parameter $S$ to a value of zero.

As has been demonstrated in Sec. III, the temperature-dependent dynamics of liquid crystals and supercooled liquids have remarkable similarities. Here we make the conjecture that the underlying physical mechanisms that give rise to the supercooled liquid dynamics are the same as those that give rise to the liquid crystal dynamics. The fundamental difference is that the liquid crystals have a true structural phase transition (isotropic to nematic) and the supercooled liquids do not. In this picture of supercooled liquids, it is envisioned that the anisotropic nature of the intermolecular interactions among the molecules produce domains with some correlation length $\xi_{sc}$, where the subscript indicates a supercooled liquid. The excitation pulse's **E** field perturbs the local structures that are the result of one or more local minima in the collective interaction potential. These local structures are not taken to be a nematiclike structure, but rather some correlation of orientation (and density) produced by the anisotropy of the interaction potential. The intermediate power law decay reflects the internal relaxation of these perturbed structures back to a local minimum of the potential surface. As with the liquid crystals, the internal relaxation does not fully remove the anisotropy. The intradomain relaxation takes the domains back to local minima. However, the **E** field has changed the local structures in an anisotropic manner. The relaxation of any domain is to the most accessible local minimum, not back to the precise initial spatial configuration. Therefore, the intradomain relaxation yields structures that still have some correlation with the **E**-field direction. This correlation is akin to the anisotropy of the local director directions that remains following intradomain relaxation in the liquid crystals. The supercooled liquid intradomain relaxation leaves a residual macroscopic anisotropy that can only decay by complete domain randomization. The complete domain randomization is the $\alpha$ relaxation, which occurs with time constant $\tau_\alpha$. Here $\tau_\alpha$ is analogous to the liquid crystal $\tau_{LdG}$. While this discussion has been in terms of the experiment, which involves the application of an **E** field, as with liquid crystals, the same picture applies to thermally induced structural fluctuations.

In a liquid crystal, as the temperature is reduced toward $T_{NI}$, the size of the pseudonematic domains ($\xi$) grows and $\tau_{LdG}$ increases, both diverging as the phase transition temperature is approached. Because $\tau_{LdG}$ reflects the time for pseudonematic domain randomization, it grows rapidly as the temperature is lowered (see Fig. 9), although the viscosity does not increase as dramatically. Supercooled liquids do not have a structural phase transition. Therefore, the structural domain growth must be arrested at some temperature on a mesoscopic length scale. The correlation length $\xi_{sc}$ (or distribution of lengths) stops increasing. Despite the fact that $\xi_{sc}$ does not diverge, the finite-sized domains can play an important role in the dynamics of supercooled liquids and the glass transition. The role of domains or structural inhomogeneities in supercooled liquid dynamics and the glass transition has been discussed by many researchers from many different perspectives.[22,23,63–73] The analogy between supercooled liquids and the isotropic phase of liquid crystals may prove useful in advancing understanding of supercooled liquids.

## ACKNOWLEDGMENT

This research was supported by the National Science Foundation Grant No. DMR-0088942.

[1] C. A. Angell, Science **267**, 1924 (1995).
[2] H. Z. Cummins, G. Li, W. Du, Y. H. Hwang, and G. Q. Shen, Suppl. Prog. Theor. Phys. **126**, 21 (1997).
[3] G. Li, M. Du, A. Sakai, and H. Z. Cummins, Phys. Rev. A **46**, 3343 (1992).
[4] G. Li, W. M. Du, X. K. Chen, and H. Z. Cummins, Phys. Rev. A **45**, 3867 (1992).
[5] J. Wuttke, M. Kiebel, E. Bartsch, F. Fujara, W. Petry, and H. Sillescu, Z. Phys. B: Condens. Matter **91**, 357 (1993).
[6] W. Petry, E. Bartsch, F. Fujara, M. Kiebel, H. Sillescu, and B. Farago, Z. Phys. B: Condens. Matter **83**, 175 (1991).
[7] M. Kiebel, E. Bartsch, O. Debus, F. Fujara, W. Petry, and H. Sillescu, Phys. Rev. B **45**, 10301 (1992).
[8] W. Steffen, A. Patkowski, H. Gläser, G. Meier, and E. W. Fischer, Phys. Rev. E **49**, 2992 (1994).
[9] R. Bergmann, L. Börjesson, L. M. Torell, and A. Fontana, Phys. Rev. B **56**, 11619 (1997).
[10] V. Krakoviack, C. Alba-Simionesco, and M. Krauzman, J. Chem. Phys. **107**, 3417 (1997).
[11] A. Tölle, H. Schober, J. Wuttke, and F. Fujara, Phys. Rev. E **56**, 809 (1997).
[12] P. Lunkenheimer, A. Pimenov, M. Dressel, Y. G. Goncharov, R. Böhmer, and A. Loidl, Phys. Rev. Lett. **77**, 318 (1996).
[13] U. Schneider, P. Lunkenheimer, R. Brand, and A. Loidl, Phys. Rev. E **59**, 6924 (1999).
[14] A. Arbe, D. Richter, J. Colmenero, and B. Farago, Phys. Rev. E **54**, 3853 (1996).
[15] M. Giordano, D. Leponini, and M. Tosi, J. Phys.: Condens. Matter **11**, A1 (1999).

[16] G. Hinze, D. D. Brace, S. D. Gottke, and M. D. Fayer, J. Chem. Phys. **113**, 3723 (2000).
[17] S. D. Gottke, G. Hinze, D. D. Brace, and M. D. Fayer, J. Phys. Chem. B **105**, 238 (2001).
[18] D. D. Brace, S. D. Gottke, H. Cang, and M. D. Fayer, J. Chem. Phys. **116**, 1598 (2002).
[19] H. Cang, V. N. Novikov, and M. D. Fayer, J. Chem. Phys. (to be published).
[20] R. Torre, P. Bartolini, M. Ricci, and R. M. Pick, Europhys. Lett. **52**, 324 (2000).
[21] R. Torre, P. Bartolini, and R. M. Pick, Phys. Rev. E **57**, 1912 (1998).
[22] M. D. Ediger, Annu. Rev. Phys. Chem. **51**, 99 (2000).
[23] H. Sillescu, J. Non-Cryst. Solids **243**, 81 (1999).
[24] W. Kob and H. C. Anderson, Phys. Rev. E **52**, 4134 (1995).
[25] S. R. Kudchadkar and J. M. Wiest, J. Chem. Phys. **103**, 8566 (1995).
[26] S. Kämmerer, W. Kob, and R. Schilling, Phys. Rev. E **56**, 5450 (1997).
[27] S. Kämmerer, W. Kob, and R. Schilling, Phys. Rev. E **58**, 2141 (1998).
[28] R. Schilling and T. Scheidsteger, Phys. Rev. E **56**, 2932 (1997).
[29] E. G. Hanson, Y. R. Shen, and G. K. L. Wong, Phys. Rev. A **14**, 1281 (1976).
[30] F. W. Deeg, S. R. Greenfield, J. J. Stankus, V. J. Newell, and M. D. Fayer, J. Chem. Phys. **93**, 3503 (1990).
[31] J. J. Stankus, R. Torre, C. D. Marshall, S. R. Greenfield, A. Sengupta, A. Tokmakoff, and M. D. Fayer, Chem. Phys. Lett. **194**, 213 (1992).
[32] S. D. Gottke, D. D. Brace, H. Cang, B. Bagchi, and M. D. Fayer, J. Chem. Phys. **116**, 360 (2002).
[33] S. D. Gottke, H. Cang, B. Bagchi, and M. D. Fayer, J. Chem. Phys. **116**, 6339 (2002).
[34] H. Cang, J. Li, and M. D. Fayer, Chem. Phys. Lett. **366**, 82 (2002).
[35] P. G. de Gennes, Phys. Lett. **30A**, 454 (1969).
[36] P. G. de Gennes, *The Physics of Liquid Crystals* (Clarendon, Oxford, 1974).
[37] G. K. L. Wong and Y. R. Shen, Phys. Rev. Lett. **30**, 895 (1973).
[38] T. D. Gierke and W. H. Flygare, J. Chem. Phys. **61**, 22331 (1974).
[39] T. W. Stinson III and J. D. Litster, Phys. Rev. Lett. **25**, 503 (1970).
[40] J. D. Litster and T. W. Stinson III, J. Appl. Phys. **41**, 996 (1970).
[41] J. C. Fillippini and Y. Poggi, Phys. Lett. **65A**, 30 (1978).
[42] W. H. de Jeu, in *Solid State Physics*, edited by L. Liebert (Academic, New York, 1978), p. 109.
[43] H. Kresse, in *Advances in Liquid Crystals*, edited by G. H. Brown (Academic, New York, 1983), Vol. 6, p. 109.
[44] J. J. Stankus, R. Torre, and M. D. Fayer, J. Phys. Chem. **97**, 9478 (1993).
[45] R. Torre and S. Californo, J. Chim. Phys. **93**, 1843 (1996).
[46] R. Torre, F. Tempestini, P. Bartolini, and R. Righini, Philos. Mag. B **77**, 645 (1998).
[47] R. S. Miller and R. A. MacPhail, Chem. Phys. Lett. **241**, 121 (1995).
[48] Y. X. Yan, L. G. Cheng, and K. A. Nelson, Adv. Infrared Raman Spectrosc. **16**, 299 (1987).
[49] Y. X. Yan and K. A. Nelson, J. Chem. Phys. **87**, 6240 (1987).
[50] Y. X. Yan and K. A. Nelson, J. Chem. Phys. **87**, 6257 (1987).
[51] F. W. Deeg, J. J. Stankus, S. R. Greenfield, V. J. Newell, and M. D. Fayer, J. Chem. Phys. **90**, 6893 (1989).
[52] W. Götze, *Liquids, Freezing and Glass Transition* (Elsevier Science, New York, 1989).
[53] W. Götze and L. Sjögren, Rep. Prog. Phys. **55**, 241 (1992).
[54] D. McMorrow, W. T. Lotshaw, and G. Kenney-Wallace, IEEE J. Quantum Electron. **24**, 443 (1988).
[55] D. McMorrow and W. T. Lotshaw, J. Phys. Chem. **95**, 10395 (1991).
[56] S. Ruhman, L. R. Williams, A. G. Joly, B. Kohler, and K. A. Nelson, J. Phys. Chem. **91**, 2237 (1987).
[57] F. W. Deeg and M. D. Fayer, J. Chem. Phys. **91**, 2269 (1989).
[58] S. Kinoshita, Y. Kai, M. Yamaguchi, and T. Yagi, Phys. Rev. Lett. **75**, 148 (1995).
[59] Y. Kai, S. Kinoshita, M. Yamaguchi, and T. Yagi, J. Mol. Liq. **65–66**, 413 (1995).
[60] W. Götze, J. Phys.: Condens. Matter **2**, 8485 (1990).
[61] G. Li, G. M. Fuchs, W. M. Du, A. Latz, N. J. Tao, J. Hernandez, W. Götze, and H. Z. Cummins, J. Non-Cryst. Solids **172**, 43 (1994).
[62] S. Ravichandran, A. Perera, M. Moreau, and B. Bagchi, J. Chem. Phys. **109**, 7349 (1998).
[63] G. Adam and J. H. Gibbs, J. Chem. Phys. **43**, 139 (1965).
[64] D. Kivelson, G. Tarjus, X. Zhao, and S. A. Kivelson, Phys. Rev. E **53**, 751 (1996).
[65] J. P. Garahan and D. Chandler, Phys. Rev. Lett. **89**, 035704 (2002).
[66] R. Bohmer, G. Hinze, G. Diezemann, B. Geil, and H. Sillescu, Europhys. Lett. **36**, 55 (1996).
[67] Y. Gebremichael, T. B. Schroder, F. W. Starr, and S. C. Glotzer, Phys. Rev. E **64**, 051503 (2001).
[68] S. C. Glotzer, V. N. Novikov, and T. B. Schroder, J. Chem. Phys. **112**, 509 (2000).
[69] C. Kaur and S. P. Das, Phys. Rev. Lett. **86**, 2062 (2001).
[70] C. Kaur and S. P. Das, Phys. Rev. Lett. **89**, 085701 2002).
[71] W. Kob, C. Donati, S. J. Plimpton, P. H. Poole, and S. C. Glotzer, Phys. Rev. Lett. **79**, 2827 (1997).
[72] F. H. Stillinger and J. A. Hodgdon, Phys. Rev. E **50**, 2064 (1994).
[73] E. Weeks, J. C. Crocker, A. C. Levitt, A. Schofield, and D. A. Weitz, Science **287**, 627 (2000).